Frontiers in Health Informatics
ISSN-Online: 2676-7104
www.healthinformaticsjournal.com
2024; Vol 13: Issue 3
Open Access

Pulsed Laser-Ablated CuO Nanoparticles and Femtosecond Laser Irradiation in Targeting Common Ocular Pathogens

Emad Neamah [1,2], Yasmin Abd El-Salam [1], Esraa Ahmed [1], Fatma Abdel-Samad [1], Ahmed O. El-Gendy [1,3 *], Ola Dabbous [4], Tarek Mohamed [1,5]

1 Laser Institute for Research and Applications LIRA, Beni-Suef University, Beni-Suef 62511, Egypt

2 Anbar Health Department, Anbar province, Ministry of Health, Iraq

3 Faculty of Pharmacy, Department of Microbiology and Immunology, Beni-Suef University, Beni-Suef 62514, Egypt

4 Department of Medical Applications of Laser, National Institute of Laser Enhanced Sciences (NILES), Cairo University, Giza, Egypt

5 Department of Engineering, Faculty of Advanced Technology and Multidiscipline, Universitas Airlangga, Indonesia

Cite this paper as: Emad Neamah, Yasmin Abd El-Salam, Esraa Ahmed, Fatma Abdel-Samad, Ahmed O. El-Gendy, Ola Dabbous, Tarek Mohamed (2024) Pulsed Laser-Ablated CuO Nanoparticles and Femtosecond Laser Irradiation in Targeting Common Ocular Pathogens. *Frontiers in Health Informatics, 13* (3),3508-3522

Abstract

Introduction: *Nanotechnology holds promise for advancing antibacterial therapies, particularly through the utilization of metal oxide nanoparticles and innovative treatment strategies.*

Objectives: This study explores the synthesis and antibacterial properties of copper oxide nanoparticles (CuO NPs) produced via Pulsed Laser Ablation in Liquids (PLAL) and their potential application in ocular infection treatments.

Methods: *CuO NPs were synthesized by irradiating a copper sample with a 532 nm nanosecond laser at varying powers (500-900 mW) for 30 minutes. The nanoparticles were characterized for their optical absorption, average size, and concentration. The antibacterial effectiveness of these nanoparticles was evaluated against both Gram-positive bacteria (Staphylococcus aureus) and Gram-negative bacteria (Pseudomonas aeruginosa). The study also evaluated the biocompatibility of CuO NPs with retinal epithelial cells (ARPE-19) using the MTT assay.*

Results: *Transmission electron microscopy (TEM) confirmed the production of CuO NPs with dimensions ranging from 4.6 to 6.5 nm. Results indicated that CuO NPs exhibit a concentration-dependent antibacterial activity which is enhanced when combined with femtosecond laser irradiation at 400 nm. Despite these antibacterial effects, the cytotoxicity of CuO NPs remains a concern, highlighting the need for further research to optimize their safety and effectiveness for clinical applications.*

Conclusions: *Optimal laser settings produced nanoparticles within the quantum dot size range, with the highest yields achieved at 900 mW power. While the antibacterial efficacy of CuO NPs shows especially when combined with femtosecond laser treatment, further studies are necessary to address safety concerns and refine production techniques for clinical viability.*

Keywords*: Eye infection; Laser ablation, antibacterial, Copper oxide nanoparticles, Biocompatibility, photodynamic therapy, Gram-positive and Gram-negative bacteria, Femtosecond laser, Quantum dots, MRSA; Pseudomonas aeruginosa*

INTRODUCTION

Nanotechnology constitutes vast and captivating domain of scientific inquiry, offering substantial advantages across a multitude of disciplines. These encompass industrial applications, medical advancements, biotechnological innovations, agricultural enhancements, electronic developments, energy solutions, and life sciences [1-6]. Recently, nanoscience has emerged as a significant research area due to ongoing efforts to create nano-sized materials using a variety of tools and techniques [7]. Nanoparticles (NPs) are a broad class of materials characterized by particles with at least one dimension smaller than 100 nm [8]. These nanoparticles have unique capabilities that depend on their size and shape, making them particularly interesting for various applications, especially in biological and medical fields such as drug delivery [9], antibacterial agents [10], cancer treatment [11], and sensing [12-14].

Severe ocular infections caused by bacteria, viruses, fungi, or parasites can result in blindness and visual impairments if left untreated [15, 16]. On an international scale, bacterial pathogens classified as either positive or negative Gram, which both cause between 32% and 74% of complications from eye infections [17, 18]. The risk of an eye infection varies depending on the type of bacterial pathogen [19]. Staphylococcus aureus and Pseudomonas aeruginosa are two of the most prevalent Gram-positive and Gram-negative bacterial isolates found in ocular infections, respectively [20, 21]. The overuse and misuse of antibacterial medications have led to a rapid increase in antibiotic-resistant bacterial pathogens [22], highlighting the need for innovative alternative antibacterial therapies [23]. Nanotechnology-based strategies are increasingly seen as a promising alternative antibacterial treatment [24].

Metal oxide nanoparticles, particularly copper oxide (CuO) NPs, have lately garnered interest for their antimicrobial capabilities, making them a promising alternative antibacterial modality [25, 26]. To enhance their effectiveness, various synthesis methods have been investigated [27]. Among these methods, Pulsed Laser Ablation in Liquids (PLAL) has gained significant attention for its one-step, high-quality preparation process [28, 29]. The PLAL technique offers several advantages, including simple and clean synthesis, ambient conditions without the need for high temperatures or special physical conditions [30], and the elimination of surfactants, which are typically required in chemical synthesis methods to create dispersed NPs [31]. The creation of nanoscale transition metal oxides such as copper oxide (CuO), iron oxide (FeO), titanium oxide (TiO2), and tin oxide (SnO2) has attracted significant interest due to their strong antibacterial activity, high thermal conductivity, and superior catalytic activity [32]. Among all metal oxides, CuO NPs have drawn the most attention due to their distinctive characteristics and applications [33-35].

Laser-based photodynamic therapy (lb-aPDT) is another potential antibacterial therapeutic method. which offers a non-invasive option for eradicating various infections [36]. Expanding on our previous research, we examine the bactericidal effectiveness of antibacterial therapies utilizing femtosecond lasers [36, 37], as well as combined therapeutic antibacterial strategies utilizing various NPs generated with PLAL [38-40].

OBJECTIVES

This research focuses on CuO NPs generated using PLAL. The study examines the effects of irradiating a copper sample with a pulsed laser at different average powers (500-900 mW) and a constant exposure time of 30 minutes. Measurements such as optical absorption, average size, and concentration of CuO NPs were performed. Moreover, the in vitro biocompatibility with retinal epithelial cells and antibacterial activity of the produced NPs have been evaluated in comparison to or in combination using femtosecond laser light at 400nm wavelength, 50 mW average power, and 159 J/cm2 energy density.

METHODS

Synthesis of CuO NPs by PLAL

A laser model of Nd: YAG (Quanta-Ray PRO-Series 350, which is a Spectra-Physics product) featuring a 10 ns pulsed duration, which stem the wavelength of 532 nm spectrum, and 10 Hz rate of repetition was utilized in the experiment shown in Fig. 1 to generate CuO NPs. CuO NPs colloidal solution was generated by exposing a rectangular piece of bulk Cu measuring 25 × 20 × 2 mm with a purity of nearly 99.99% to the pulsed laser. Before the ablation procedure, the sample underwent polishing to remove the oxide layer formed from exposure to air, ensuring the bulk surface was smooth and free of protrusions. Subsequently, the sample was subjected to ultrasonic cleaning with alcohol and ethanol for thirty minutes to eliminate any remaining organic residues. After being cleaned, the sample was put in a glass container with about 10 mL of distilled water. In order to avoid the laser beam from staying focused on the same point and ensure uniform ablation, the beaker was subsequently mounted on a rotating apparatus that spun both the target and the water that had been distilled. To aim the laser beam at the sample, mirrors and a 10.5 cm focal length convex lens were employed. were applied, and the sample was positioned nearly in the lens's focus.

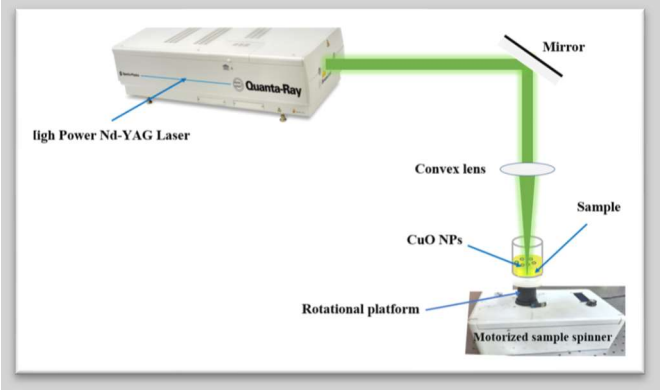

Figure 1: Apparatus used in the experiment for producing CuO nanoparticles using pulsed laser ablation in water.

Laser Ablated CuO Nanoparticles Characterization

Using a spectrophotometer (Model: C-7200), the synthesized samples' UV-visible absorption spectra were ascertained. The morphology and size of the CuO nanoparticles (NPs) were analyzed via transmission electron microscopy (TEM). TEM images were utilized for size distribution measurements of each sample. The concentration of the synthesized NPs was quantified employing ICP-OES with synchronized vertical dual view (SVDV) configuration using an Agilent 5100 instrument equipped with a Vapor Generator Accessory (VGA 77).

Microorganism and Culture Conditions.

The study examined two types of bacterial pathogenic organisms: Gram-negative *P. aeruginosa* (ATCC 9027) and Gram-positive *Staphylococcus aureus*, or MRSA (ATCC 43300). Both cultures were cultivated in Brain Heart Infusion (BHI) broth at 37°C. Prior to treatment, the microbial suspension's optical density was standardized to 0.5 McFarland standard, corresponding to approximately 1.5×108 colony forming units (CFU/mL). Subsequently, 100 µL aliquots of the standardized suspensions were dispensed into designated wells of a 96-well microtiter plate.

Femtosecond laser system preparation and treatment of bacterial pathogens

In this investigation, a femtosecond-locked Ti: sapphire laser with an 80 MHz repetitive rate, a typical power level of 1.5–2.9 W, and wavelengths spanning from 690 to 1040 nm was employed (MAI TAI HP, Spectra-Physics). This laser apparatus pumped Femtosecond pulses at 400 nm in wavelength were generated by the Spectra-Physics INSPIRE HF100

laser system.

The output power of the laser was measured using a Newport 843R power meter. The distance of the laser's beam was 10 cm over the 96-well microtiter plate containing the overnight-cultured microbial organisms as shown in Fig. 2. Initially, the beam diameter was expanded from 2 mm to 10 mm using a beam expander composed of two converging lenses. Although the adjustable iris (designated as I) was used to modify the laser beam's diameter, the laser attenuator (labeled as A) was used to reduce the laser power that reached the samples to 50 mW. Laser beam focus on the samples was achieved by means of mirrors M1 and M2.

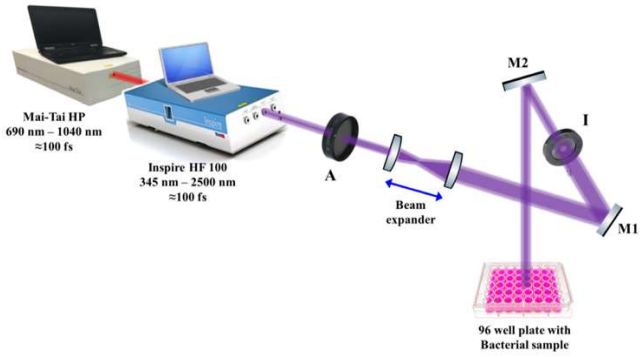

Figure 2: The experimental configuration aims to expose bacteria to femtosecond laser radiation. The laser beam was directed towards the samples using the highly reflecting mirrors M1 and M2. The laser power that reached the samples was modulated using an attenuator (designated as A), with a setting of 50 mW for this particular experiment. The laser beam's diameter was adjusted via an iris (designated as I) that could be adjusted.

Assessment of Growth Kinetics in Gram-Positive and Gram-Negative Bacterial Pathogens Following Femtosecond Laser and/or CuO NPs Treatments

CuO nanoparticles (NPs) were vortexed at specified concentrations in double-strength BHI broth. Subsequently, 100 µL of this mixture was added to each well of a 96-well microtiter plate. Using a multichannel pipette, 100 µL aliquots of prepared bacterial cultures, whether laser-treated or untreated (control), were then added to the plate. Each well of the microtiter plate contained bacterial suspensions treated as follows: Laser Treatment, where microorganisms were exposed to femtosecond laser pulses; CuO NPs Treatment, involving the addition of CuO NPs dispersed in BHI broth to bacterial cultures; and Combined Treatment, where bacterial cultures received both laser treatment and CuO NPs simultaneously. While the negative control wells contained only BHI broth, the positive control wells contained untreated microorganisms. The plate was treated and then incubated for 16 hours at 37°C. Every thirty minutes throughout the incubation phase, data was gathered and each well's optical density (OD) was determined using a microplate reader calibrated to 620 nm.

Growth curve and growth rate analysis (µmax) were determined to validate the possible antibacterial effect of CuO NPs. The following equation was used to obtain µmax , in where t is the time at which µmax was reached, Xt is the growth absorbance at a given time point, and X0 is the initial growth absorbance. $Xt = X0 \exp(\mu max \cdot t)$

Biocompatibility of CuO NPs with ARPE-19 cells evaluated by MTT assay

The MTT method was used to examine the metabolic process of the adult retinal pigment epithelial cell line (ARPE-19) in order to evaluate the biocompatibility of produced CuO nanoparticles (NPs). This colorimetric method relies on the reduction of 3-(4,5-dimethylthiazol-2-yl)-2,5-diphenyltetrazolium bromide (MTT), a yellow tetrazolium salt, to purple formazan crystals by metabolically active cells. ARPE-19 cells were cultured in T-75 tissue culture flasks supplemented with 10% v/v fetal bovine serum and 1% antibiotic-antimycotic solution, along with RPMI 1640 medium. The cells were

cultured for 48 hours at 37°C in a CO2 incubator before being separated using trypsin. Then, cells were sown at a density of 4 x 104 cells/cm2 into a 96-well microtiter plate (100 µL/well). After overnight incubation to enhance adhesion, the cell monolayer was subjected to a two-fold multiple dilution of CuO NPs and cultured for an additional day at 37°C in CO2 incubators.

After the incubation period, cellular morphology changes due to CuO NPs treatment were assessed using a phase-contrast inverted microscope. After that, the cells were treated with an MTT solution (0.5 mg/mL) for 4 hours at 37 °C. Following removing excess medium, the formazan generated by metabolically active cells were dissolved in DMSO, and the intensity of absorption was determined at 570 nm using a plate microtiter analyzer. To calculate the proportions of cytotoxicity and cell viability, the following formulas were utilized:

% cytotoxicity = 1 – (mean absorbance of treated cells/mean absorbance of control).

% viability = 100 - % cytotoxicity.

Statistical analysis

Data analysis included plotting growth curves to monitor microbial proliferation over time, followed by assessing growth rates and kinetics. Mean values ± standard error were utilized for data representation. Tukey's post hoc test and one-way ANOVA were carried out using GraphPad Prism 7 software for statistical analyses compared to multiple groups. Statistical significance was set at $P < 0.05$. Within a class II biological safety cabinet (MSC-Advantage™), a sterile laminar flow hood, the experimental procedures were carried out in triplicate.

Lorem ipsum dolor sit amet, consectetur adipiscing elit, sed do eiusmod tempor incididunt ut labore et dolore magna aliqua. Orci a scelerisque purus semper eget duis at tellus at. Quisque egestas diam in arcu cursus. Pulvinar mattis nunc sed blandit. Tempus iaculis urna id volutpat lacus laoreet non curabitur. Morbi tincidunt ornare massa eget egestas purus viverra accumsan in. Vehicula ipsum a arcu cursus. Sapien et ligula ullamcorper malesuada proin. Ut diam quam nulla porttitor. Tincidunt dui ut ornare lectus sit. Neque ornare aenean euismod elementum nisi quis eleifend. Mus mauris vitae ultricies leo integer. In nulla posuere sollicitudin aliquam ultrices. Eget duis at tellus at urna condimentum mattis. Tellus molestie nunc non blandit. Quam quisque id diam vel quam elementum pulvinar. Integer quis auctor elit sed vulputate mi. Pellentesque elit eget gravida cum sociis natoque penatibus et. Aliquet risus feugiat in ante. Commodo ullamcorper a lacus vestibulum sed.

Congue nisi vitae suscipit tellus mauris a diam maecenas. Aliquet nec ullamcorper sit amet risus. Pulvinar sapien et ligula ullamcorper malesuada proin libero nunc consequat. Non consectetur a erat nam at lectus urna duis convallis. Purus viverra accumsan in nisl nisi scelerisque eu. Netus et malesuada fames ac turpis egestas maecenas pharetra convallis. Sed turpis tincidunt id aliquet. Et malesuada fames ac turpis egestas sed tempus urna et. In dictum non consectetur a erat nam at. Nulla aliquet porttitor lacus luctus accumsan tortor posuere. Nunc consequat interdum varius sit amet mattis vulputate enim nulla. Cras tincidunt lobortis feugiat vivamus. Venenatis a condimentum vitae sapien pellentesque habitant morbi. Suscipit adipiscing bibendum est ultricies integer. Et ultrices neque ornare aenean. Ut porttitor leo a diam sollicitudin tempor id eu. Lorem ipsum dolor sit amet consectetur adipiscing elit. Morbi tincidunt ornare massa eget egestas purus viverra accumsan in. Sit amet consectetur adipiscing elit duis tristique.

Ipsum dolor sit amet consectetur adipiscing. Arcu felis bibendum ut tristique. Lectus sit amet est placerat in egestas. In massa tempor nec feugiat nisl pretium. Vel pharetra vel turpis nunc eget lorem dolor. Ornare aenean euismod elementum nisi quis eleifend quam. Tellus id interdum velit laoreet id donec. Eget arcu dictum varius duis at consectetur lorem donec massa. Amet facilisis magna etiam tempor orci eu lobortis. Consectetur adipiscing elit duis tristique sollicitudin. Pellentesque dignissim enim sit amet venenatis urna cursus eget.

Pellentesque adipiscing commodo elit at imperdiet. Lectus proin nibh nisl condimentum id venenatis. Dignissim diam quis enim lobortis scelerisque fermentum dui faucibus in. Volutpat diam ut venenatis tellus. Vehicula ipsum a arcu cursus vitae. Volutpat maecenas volutpat blandit aliquam etiam. Sed id semper risus in. Eget nulla facilisi etiam dignissim diam quis

enim lobortis scelerisque. Tellus in hac habitasse platea dictumst. Non enim praesent elementum facilisis leo. A cras semper auctor neque vitae tempus quam pellentesque. Dolor magna eget est lorem ipsum dolor sit amet consectetur.

Neque laoreet suspendisse interdum consectetur libero id faucibus. Ac turpis egestas maecenas pharetra convallis. Sagittis aliquam malesuada bibendum arcu vitae elementum curabitur vitae nunc. Nulla facilisi cras fermentum odio eu feugiat pretium nibh. Tortor at auctor urna nunc id cursus. Bibendum enim facilisis gravida neque convallis a cras semper auctor. Feugiat vivamus at augue eget arcu. Et netus et malesuada fames ac turpis egestas. Quisque id diam vel quam elementum. Amet est placerat in egestas erat. Egestas maecenas pharetra convallis posuere morbi leo. Sagittis aliquam malesuada bibendum arcu vitae. Ultricies lacus sed turpis tincidunt id aliquet risus. Ipsum dolor sit amet consectetur adipiscing elit. Cursus sit amet dictum sit amet justo donec.

RESULTS & DISCUSSION

The color of CuO nanoparticles (NPs) prepared by pulsed laser ablation in liquid is shown in Fig. 3. The color variation was generated due to the high absorption and light scattering induced by the CuO NPs. The absorption and scattering impacts are highly dependent on the concentration of the created NPs as illustrated in Fig. 3. Due to the ablation producer, the solutions gained an olive color, which is attributed to the presence of CuO nanoparticles. It was found that intensity of the olive color varied with an average power which may indicate that the optical characteristics also depend on particle density. The UV-absorption spectrum of CuO nanoparticles (NPs) is illustrated in Fig. 4, determined using a spectrophotometer (Model: C-7200). The surface plasmon resonance (SPR) of CuO NPs absorption peaks appears in the range of 200–300 [41]. This figure shows the effects of different average powers (500-900) mW at a constant exposure time of 30 min. Moreover, it was observed that with increased average power from 500 mW to 900 mW, the intensity of the absorption peaks exhibited to be greater. The increase of peak absorbance indicates that the concentration of CuO nanoparticles increased, additionally, the intensity of color increased.

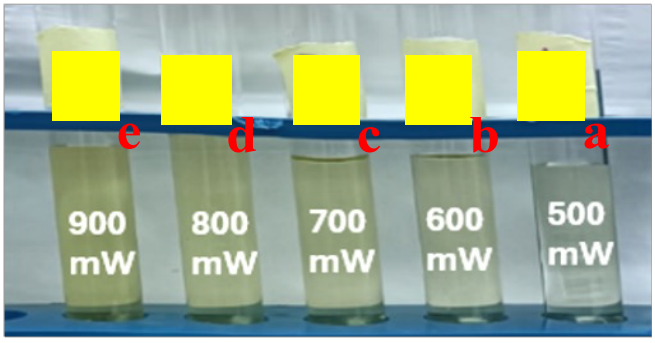

Figure 3: CuO NPs colloidal solutions were synthesized by pulsed laser ablation in liquid at a constant exposure duration of 30 minutes with varying average laser powers: (a) 500 mW, (b) 600 mW, (c) 700 mW, (d) 800 mW, and (e) 900 mW.

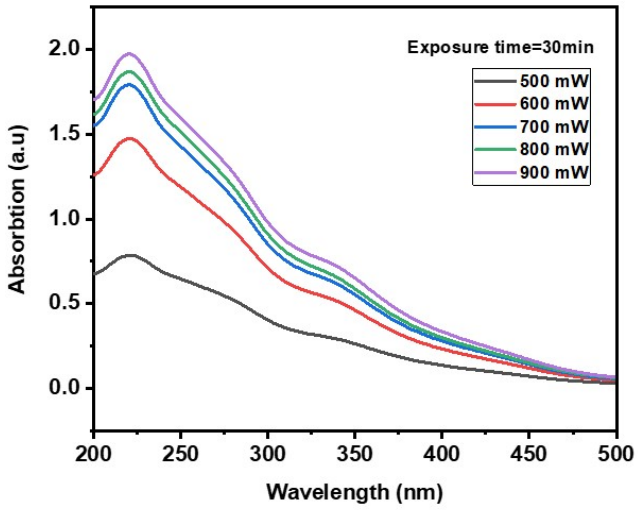

Figure 4: UV/Vis absorption spectrum of CuO NPs synthesized via pulsed laser ablation at different average powers (500-900 mW).

The CuO nanoparticles (NPs) were analyzed for their structure and average size using a 200 kV transmission electron microscope (HR-TEM, JEM-2100, Joel, Japan). A little amount of the colloidal solution was placed onto a copper grid that had been coated using carbon, and the grid was left to dry at room temperature to prepare the samples for TEM investigation. The diameters of several dispersed particles were measured in TEM images using the software ImageJ to estimate the particle size [42]. Fig. 5 illustrates the size distribution histogram of CuO NPs colloidal solutions prepared by pulsed laser ablation at various average powers (500-900 mW) with a constant exposure time of 30 minutes. The TEM images of colloidal CuO NPs created by pulsed laser ablation, shown in the insets of Fig. 5a-e, confirm that the synthesized CuO NPs were spherical. When the Cu sample was exposed to average powers of 500, 600, 700, 800, and 900 mW, the average sizes of the CuO NPs were 6.5, 6.0, 5.7, 5.6, and 4.6 nm, respectively.

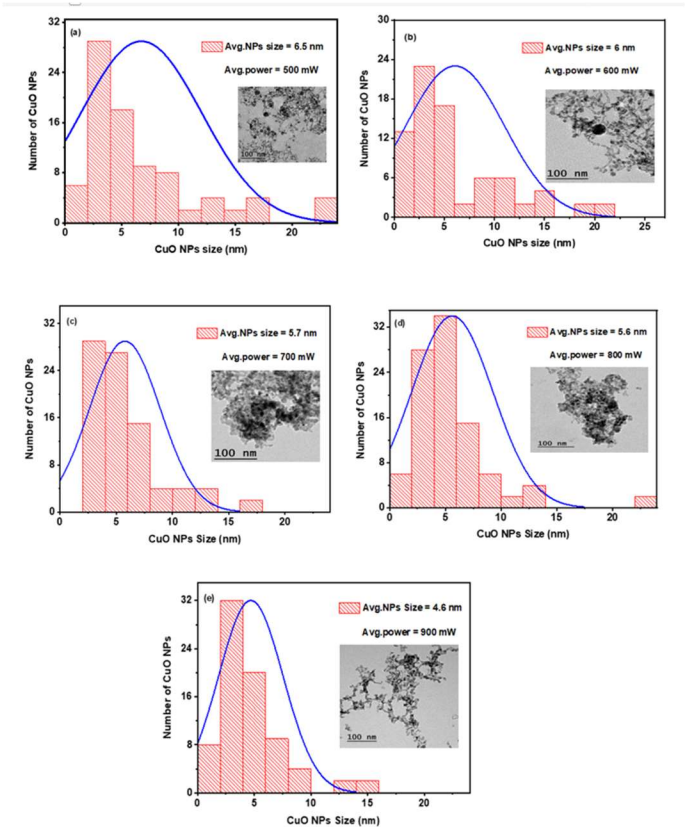

Figure 5: Histogram showing the size distribution of CuO NPs colloidal solutions synthesized at different average powers: (a) 500 mW, (b) 600 mW, (c) 700 mW, (d) 800 mW, and (e) 900 mW, with a constant exposure time of 30 minutes. TEM images demonstrating the morphology of the synthesized CuO NPs are inset in panels (a)-(e).

The relationship between the variation in average NP size and various average powers (500-900 mW) at a constant exposure time of 30 minutes is plotted in Fig. 6. The figure demonstrates that as the average power increases from 500 mW to 900 mW, the average nanoparticle sizes decrease from 6.5 nm to 4.6 nm. This trend illustrates the fragmentation mechanism observed in nanoparticle sizes with increasing average power [38, 43, 44].

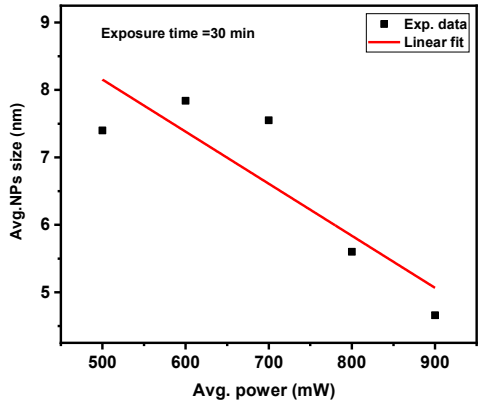

Figure 6: Variation in the average size of CuO NPs with different average powers (500-900 mW) at a constant exposure

time of 30 minutes.

Using an Agilent 5100 Synchronous Vertical Dual View (SVDV) ICP-OES and an Agilent Vapor Generation Accessory VGA 77, an inductively coupled plasma was used to quantify the amount of CuO NPs produced by pulsed laser ablation in water. The effect of different average powers on the concentration of CuO NPs colloidal is shown in Fig. 7. The figure demonstrates that the concentration of CuO NPs colloidal increased with the average power. As mentioned in Fig. 4, the increase in absorption intensity and solution color intensity of CuO NPs indicates a rise in the concentration of CuO NPs. The concentrations are 13.2, 14, 22.6, 32, and 50 mg/L at average powers of 500, 600, 700, 800, and 900 mW, respectively, with a constant exposure time of 30 minutes. Increasing the exposure of the copper sample to a higher average power of 900 mW resulted in a concentration of CuO NPs suspended in distilled water reaching 50 mg/L, compared to the lower concentrations at reduced average powers.

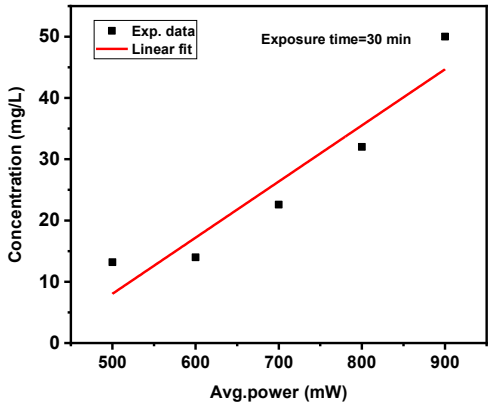

Figure 7: Variation in the concentration of CuO NPs with different average powers (500-900 mW) at a constant exposure time of 30 minutes.

Our latest study [45] investigated the impact of lb-aPDT on the growth kinetics of Staphylococcus aureus. We studied the possibility of increasing therapeutic efficacy by femtosecond laser parameter adjustment. A 15-minute exposure to a femtosecond laser at 390 nm or 400 nm wavelengths, with an average power output of 50 mW, was shown to cause a significant decrease in bacterial viability. In this study, we subjected different microbial cultures to a 400 nm femtosecond laser, delivering an energy density of 159 J/cm². This wavelength, situated within the visible spectrum, is regarded as safer for therapeutic use compared to shorter wavelengths [46, 47]. These results indicate that the 400 nm wavelength is a promising candidate for clinical applications. The antibacterial effects of lasers and other light-based technologies are generally attributed to the production of reactive oxygen species (ROS), which serve as the primary mediators of the antimicrobial activity observed at specific wavelengths. ROS are byproducts of cellular oxidative metabolism and, at optimal levels, benefit cellular functions [48]. However, external stimuli can significantly increase ROS levels [48], and excessive amounts of ROS can have detrimental effects on cell differentiation, signaling, and viability [49].

The impact of a 400 nm femtosecond laser and/or CuO nanoparticles (NPs), synthesized via laser ablation at different energies, on the growth of Methicillin-resistant Staphylococcus aureus (MRSA) and Pseudomonas aeruginosa was investigated. As depicted in Fig. 8, we analyzed the effects of CuO NPs with varying sizes: sample (a) with an average size of 6.5 nm, sample (b) with 6.0 nm, sample (c) with 5.7 nm, sample (d) with 5.6 nm, and sample (e) with 4.6 nm, all at a fixed concentration of 13.2 µg/mL.

The growth kinetics of S. aureus and P. aeruginosa were assessed, as shown in Fig. 9. Cultures treated with the laser exhibited markedly slower growth and significantly reduced growth kinetics (Y-axis) compared to untreated control cultures (X-axis), with a P-value < 0.0001. These results demonstrate that laser irradiation effectively suppressed the

growth kinetics of both pathogens in vitro. In contrast, the NPs treatment alone did not produce a significant effect, likely due to the relatively low concentration of 13.2 µg/mL used in this study [50, 51].

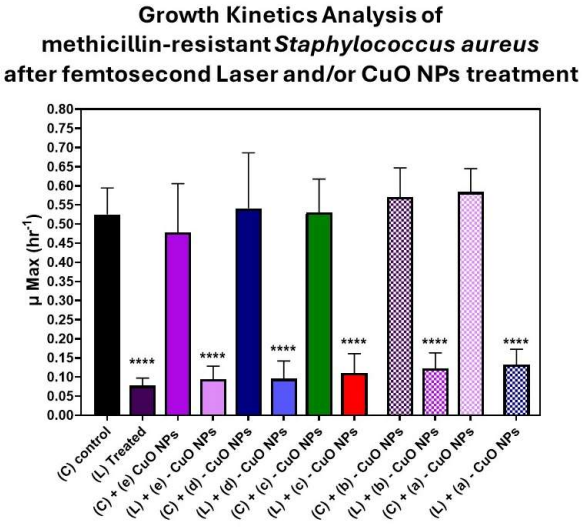

Figure 8: The bar graph presents the growth kinetics of methicillin-resistant Staphylococcus aureus (MRSA), comparing the log-phase growth rates of control cultures (C) with those subjected to different treatments: laser treatment (L), CuO NP treatment (C + a, b, c, d, or e), and combined laser and CuO NP treatment (L + a, b, c, d, or e). The femtosecond laser operated at a wavelength of 400 nm, with an average power of 50 mW applied for 15 minutes. Five distinct samples of CuO NPs were used: sample (a) with an average size of 6.5 nm, sample (b) with 6.0 nm, sample (c) with 5.7 nm, sample (d) with 5.6 nm, and sample (e) with 4.6 nm, each at a concentration of 13.2 µg/mL. Statistical significance was assessed using ANOVA followed by Tukey's test (**** $P < 0.0001$, *** $P < 0.001$, ** $P < 0.01$, * $P < 0.05$).

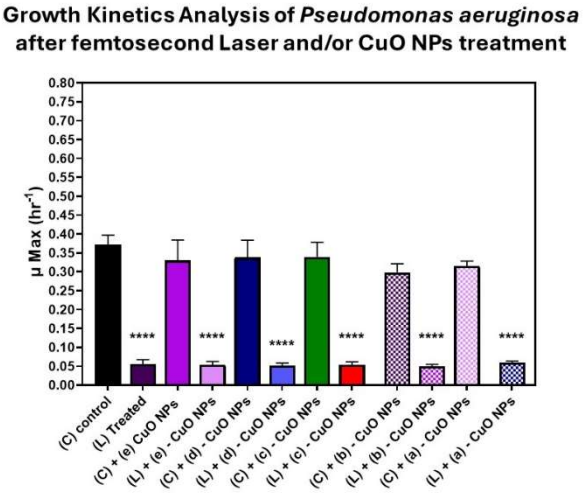

Figure 9: The bar graph illustrates the growth kinetics of Pseudomonas aeruginosa, comparing the log-phase growth rates of control cultures (C) with those subjected to different treatments: laser treatment (L), CuO NP treatment (C + a, b, c, d, or e), and combined laser and CuO NP treatment (L + a, b, c, d, or e). The femtosecond laser was applied at a wavelength of 400 nm with an average power of 50 mW for 15 minutes. Cultures were treated with five different samples of CuO NPs:

sample (a) with an average size of 6.5 nm, sample (b) with 6.0 nm, sample (c) with 5.7 nm, sample (d) with 5.6 nm, and sample (e) with 4.6 nm, each at a concentration of 13.2 µg/mL. Statistical significance was evaluated using ANOVA followed by Tukey's test (**** P < 0.0001, *** P < 0.001, ** P < 0.01, * P < 0.05).

Seeking enhancement of the CuO NPs' antibacterial efficacy we studied the photoactivation of CuO NPs, sample (e), by exposing them to femtosecond laser prior to addition to the tested pathogens. The irradiation parameters used for photoactivation were almost the same exposure parameters of the experiment except the wavelength, which was selected to be 370 nm, a wavelength included in the absorption spectrum of the prepared sample as shown before in Fig. 4, and the bacterial Growth kinetics after treated with these photoactivated NPs were compared to nonactivated ones as shown in Fig, 10. Again the effect of CuO NPs was not evident which could be attributed to their low concentration of 13.2 µg/mL.

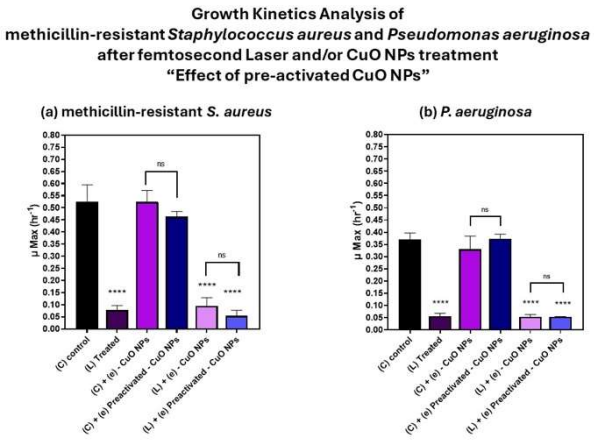

Figure 10: The bar graph shows the growth kinetics of (a) methicillin-resistant Staphylococcus aureus and (b) Pseudomonas aeruginosa, comparing the log-phase growth rates of control cultures (C) with those treated under various conditions: laser treatment (L), CuO NP treatment (C + e), laser + CuO NP treatment (L + e), and preactivated CuO NPs. The femtosecond laser was applied at a wavelength of 400 nm with an average power of 50 mW for 15 minutes. Cultures were exposed to a selected sample of CuO NPs (sample e) with an average size of 4.6 nm, all at a concentration of 13.2 µg/mL. Statistical significance was determined using ANOVA followed by Tukey's test (**** P < 0.0001, *** P < 0.001, ** P < 0.01, * P < 0.05).

At a laser ablation power of 900 mW, CuO nanoparticles (NPs) were produced at higher concentrations (~50 µg/mL in sample (e)). The effect of gradually increasing these concentrations on the growth kinetics of S. aureus and P. aeruginosa was tested, as depicted in Fig. 11. The figure shows that the antibacterial effect of CuO NPs increases with higher concentrations for both pathogens. Similar conclusions were drawn from laser-treated samples; however, the impact of femtosecond laser treatment on the growth kinetics of both pathogens was so pronounced that it overshadowed the effect of combined therapy.

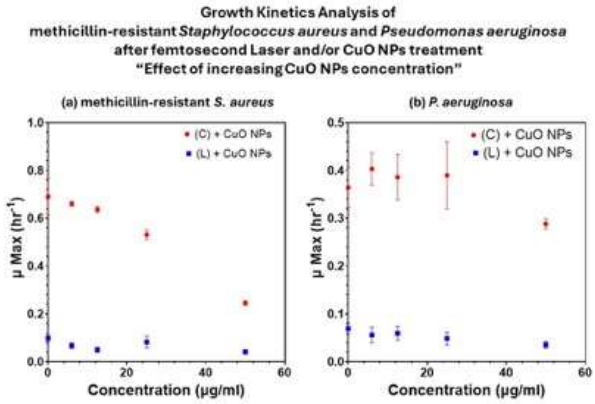

Figure 11: The graph illustrates the growth kinetics of (a) methicillin-resistant Staphylococcus aureus and (b) Pseudomonas aeruginosa. It compares the growth rates during the logarithmic phase between control cultures (C) and those subjected to laser treatment (L) with varying concentrations (0, 6.25, 12.5, 25, and 50 µg/mL) of CuO nanoparticles (NPs) with an average size of 4.6 nm. The femtosecond laser treatment was administered at a wavelength of 400 nm with an average power of 50 mW for a duration of 15 minutes. Statistical significance was assessed using ANOVA followed by Tukey's test (**** $P < 0.0001$, *** $P < 0.001$, ** $P < 0.01$, * $P < 0.05$).

Overall, CuO NPs in a concentration-dependent consequence could show antimicrobial tendence against both Gram-positive and Gram-negative pathogens exhibiting a "contact-killing" mechanism. This mechanism was previously observed in different studies [52-54]. We can recommend using parameter 900 mW for the preparation of CuO NPs by PLAL as it gives higher concentrations with even smaller sizes for further antibacterial investigations. However, seeking an alternative treatment should highlight the biocompatibility of the approach for a successful clinical application. Hence the biocompatibility of the freshly produced CuO NPs by PLAL was tested with retinal epithelial cells ARPE-19 cells evaluated by MTT assay as shown in Fig. 12. As widely known, the cytotoxic effects of CuO NPs are a huge concern which was also evident in our study with variations that could be attributed to the variation of the final concentration of each sample.

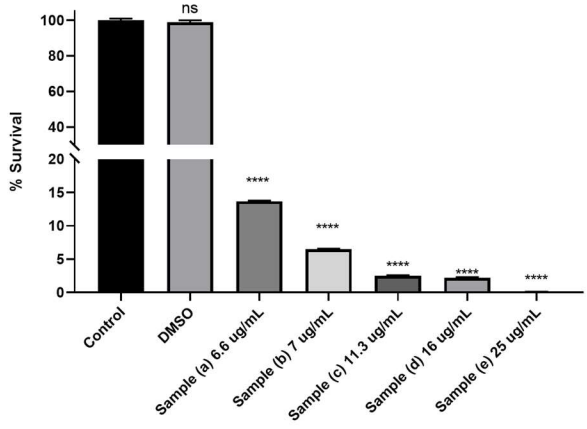

Figure 12: The bar graph shows the survival percentage of ARPE-19 cells following exposure to different concentrations of freshly prepared CuO nanoparticles synthesized via pulsed laser ablation in liquid (PLAL). Statistical significance was determined using ANOVA with subsequent Tukey's test (**** $P < 0.0001$, *** $P < 0.001$, ** $P < 0.01$, * $P < 0.05$).

Our findings suggest that combining femtosecond laser and CuO NPs might greatly inhibit bacterial growth in all tested bacteria, potentially minimizing their harmful impacts in many scenarios. Using CuO NPs as an alternative antibacterial modality is still a trade of between the higher effects with increasing concentration and the safety concerns of this approach even with PLAL synthesis method that is why research proposals like the preparation of alloy nanoparticles are being investigated to mask the toxicity while enabling the effect to take place, which will be the focus of our following research investigations [55, 56].

CONCLUSIONS

This study introduces a new perspective on the synthesis of CuO NPs using the pulsed laser ablation technique and their potential for treating various ocular infections. The physicochemical properties of nanoparticles produced by PLAL are significantly influenced by preparation conditions and laser parameters. Our research demonstrates that using a 532 nm, 10 Hz nanosecond laser system with laser power ranging from 500 to 900 mW and a constant exposure duration of 30 minutes, CuO NPs consistently maintained particle sizes within the range of quantum dots (4.6 - 6.5 nm). Notably, the highest concentration of CuO NPs was achieved at a laser power of 900 mW. Our findings indicate that CuO NPs exhibit a concentration-dependent antibacterial activity against both Gram-positive and Gram-negative bacteria, either independently at higher concentrations or in combination with femtosecond laser treatment at 400 nm. However, the safety and long-term effects of CuO NPs on the body remain major barriers to their clinical use, underscoring the need for continued research into novel or modified NP production methods.REFRENCES

[1] C. I. Moraru, C. P. Panchapakesan, Q. Huang, P. Takhistov, S. Liu, and J. L. Kokini, “Nanotechnology: a new frontier in food science,” 2003.
[2] P. M. G. Nair and I. M. %J B. trace element research Chung, “A mechanistic study on the toxic effect of copper oxide nanoparticles in soybean (Glycine max L.) root development and lignification of root cells,” vol. 162, pp. 342–352, 2014.
[3] M. H. Siddiqui, M. H. Al-Whaibi, M. Firoz, M. Y. %J N. Al-Khaishany, plant sciences: nanoparticles, and their impact on plants, “Role of nanoparticles in plants,” pp. 19–35, 2015.
[4] D. K. Tripathi *et al.*, “Nitric oxide ameliorates zinc oxide nanoparticles phytotoxicity in wheat seedlings: implication of the ascorbate–glutathione cycle,” vol. 8, p. 1, 2017.
[5] D. K. Tripathi *et al.*, “An overview on manufactured nanoparticles in plants: uptake, translocation, accumulation and phytotoxicity,” vol. 110, pp. 2–12, 2017.
[6] A. Selmani, D. Kovačević, K. %J A. in colloid Bohinc, and interface science, “Nanoparticles: From synthesis to applications and beyond,” vol. 303, p. 102640, 2022.
[7] Y. Herbani, R. S. Nasution, F. Mujtahid, and S. Masse, “Pulse laser ablation of Au, Ag, and Cu metal targets in liquid for nanoparticle production,” in *Journal of Physics: Conference Series*, IOP Publishing, 2018, p. 12005.
[8] S. Laurent *et al.*, “Magnetic iron oxide nanoparticles: synthesis, stabilization, vectorization, physicochemical characterizations, and biological applications,” vol. 108, no. 6, pp. 2064–2110, 2008.
[9] M. Arruebo, R. Fernández-Pacheco, M. R. Ibarra, and J. %J N. today Santamaría, “Magnetic nanoparticles for drug delivery,” vol. 2, no. 3, pp. 22–32, 2007.
[10] M. Raffi *et al.*, “Antibacterial characterization of silver nanoparticles against E. coli ATCC-15224,” vol. 24, no. 2, pp. 192–196, 2008.
[11] P. K. Jain, I. H. El-Sayed, and M. A. %J nano today El-Sayed, “Au nanoparticles target cancer,” vol. 2, no. 1, pp. 18–29, 2007.
[12] G. Doria *et al.*, “Noble metal nanoparticles for biosensing applications,” vol. 12, no. 2, pp. 1657–1687, 2012.
[13] K.-S. Lee and M. A. %J T. J. of P. C. B. El-Sayed, “Gold and silver nanoparticles in sensing and imaging: sensitivity of plasmon response to size, shape, and metal composition,” vol. 110, no. 39, pp. 19220–19225, 2006.
[14] X. Luo, A. Morrin, A. J. Killard, M. R. %J E. A. I. J. D. to F. Smyth, and P. A. of Electroanalysis, “Application of nanoparticles in electrochemical sensors and biosensors,” vol. 18, no. 4, pp. 319–326, 2006.
[15] M. Teweldemedhin, H. Gebreyesus, A. H. Atsbaha, S. W. Asgedom, and M. Saravanan, “Bacterial profile of ocular infections: a systematic review,” *BMC Ophthalmol.*, vol. 17, no. 1, p. 212, 2017, doi: 10.1186/s12886-017-0612-2.
[16] C. Long, B. Liu, C. Xu, Y. Jing, Z. Yuan, and X. Lin, “Causative organisms of post-traumatic endophthalmitis: a 20-year retrospective study,” *BMC Ophthalmol.*, vol. 14, no. 1, p. 34, Dec. 2014, doi: 10.1186/1471-2415-14-34.

[17] M. Teweldemedhin, M. Saravanan, A. Gebreyesus, and D. Gebreegziabiher, "Ocular bacterial infections at Quiha Ophthalmic Hospital, Northern Ethiopia: an evaluation according to the risk factors and the antimicrobial susceptibility of bacterial isolates," *BMC Infect. Dis.*, vol. 17, no. 1, p. 207, 2017, doi: 10.1186/s12879-017-2304-1.

[18] H. Hiroshi Toshida *et al.*, "Prevalence of drug resistance and culture-positive rate among microorganisms isolated from patients with ocular infections over a 4-year period," *Clin. Ophthalmol.*, p. 695, Apr. 2013, doi: 10.2147/OPTH.S43323.

[19] K. Vaziri, S. G. Schwartz, K. Kishor, and H. W. %J C. ophthalmology Flynn Jr, "Endophthalmitis: state of the art," pp. 95–108, 2015.

[20] A. D. Khosravi, M. Mehdinejad, and M. Heidari, "Bacteriological findings in patients with ocular infection and antibiotic susceptibility patterns of isolated pathogens.," *Singapore Med. J.*, vol. 48, no. 8, pp. 741–3, Aug. 2007, [Online]. Available: http://www.ncbi.nlm.nih.gov/pubmed/17657382

[21] "Profile of Microbial Isolates in Ophthalmic Infections and Antibiotic Susceptibility of the Bacterial Isolates: A Study in an Eye Care Hospital, Bangalore," *J. Clin. DIAGNOSTIC Res.*, 2014, doi: 10.7860/JCDR/2014/6852.3910.

[22] W. Gao and L. Zhang, "Nanomaterials arising amid antibiotic resistance," *Nat. Rev. Microbiol.*, vol. 19, no. 1, pp. 5–6, Jan. 2021, doi: 10.1038/s41579-020-00469-5.

[23] J. M. V. Makabenta, A. Nabawy, C.-H. Li, S. Schmidt-Malan, R. Patel, and V. M. Rotello, "Nanomaterial-based therapeutics for antibiotic-resistant bacterial infections," *Nat. Rev. Microbiol.*, vol. 19, no. 1, pp. 23–36, Jan. 2021, doi: 10.1038/s41579-020-0420-1.

[24] G. Libralato, E. Galdiero, A. Falanga, R. Carotenuto, E. de Alteriis, and M. Guida, "Toxicity Effects of Functionalized Quantum Dots, Gold and Polystyrene Nanoparticles on Target Aquatic Biological Models: A Review," *Molecules*, vol. 22, no. 9, p. 1439, Aug. 2017, doi: 10.3390/molecules22091439.

[25] M. Amiri, Z. Etemadifar, A. Daneshkazemi, and M. Nateghi, "Antimicrobial Effect of Copper Oxide Nanoparticles on Some Oral Bacteria and Candida Species.," *J. Dent. Biomater.*, vol. 4, no. 1, pp. 347–352, Mar. 2017, [Online]. Available: http://www.ncbi.nlm.nih.gov/pubmed/28959764

[26] M. Vincent, R. E. Duval, P. Hartemann, and M. Engels-Deutsch, "Contact killing and antimicrobial properties of copper," *J. Appl. Microbiol.*, vol. 124, no. 5, pp. 1032–1046, May 2018, doi: 10.1111/jam.13681.

[27] E. Moschini, G. Colombo, G. Chirico, G. Capitani, I. Dalle-Donne, and P. Mantecca, "Biological mechanism of cell oxidative stress and death during short-term exposure to nano CuO," *Sci. Rep.*, vol. 13, no. 1, p. 2326, 2023, doi: 10.1038/s41598-023-28958-6.

[28] K. S. Khashan, F. A. Abdulameer, M. S. Jabir, A. A. Hadi, G. M. %J A. in N. S. N. Sulaiman, and Nanotechnology, "Anticancer activity and toxicity of carbon nanoparticles produced by pulsed laser ablation of graphite in water," vol. 11, no. 3, p. 35010, 2020.

[29] M. Jawaid, S. %J A. S. Siengchin, and E. Progress, "Hybrid composites: A versatile materials for future," vol. 12, no. 4, p. 223, 2019.

[30] G. W. %J P. in M. S. Yang, "Laser ablation in liquids: Applications in the synthesis of nanocrystals," vol. 52, no. 4, pp. 648–698, 2007.

[31] S. V. Rao, G. K. Podagatlapalli, S. %J J. of nanoscience Hamad, and nanotechnology, "Ultrafast laser ablation in liquids for nanomaterials and applications," vol. 14, no. 2, pp. 1364–1388, 2014.

[32] D. P. Jeba, P. Ramkumar, A. David, and J. %J E. C. S. T. Ashli, "Synthesis of Green and Pure Copper Oxide Nanoparticles Using Millettia Pinnata Leaf Extract and Their Characterisation," vol. 107, no. 1, p. 17335, 2022.

[33] S. K. Yip and J. A. %J P. review letters Sauls, "Nonlinear Meissner effect in CuO superconductors," vol. 69, no. 15, p. 2264, 1992.

[34] A. Umar, M. M. Rahman, A. Al-Hajry, and Y.-B. %J E. C. Hahn, "Enzymatic glucose biosensor based on flower-shaped copper oxide nanostructures composed of thin nanosheets," vol. 11, no. 2, pp. 278–281, 2009.

[35] Y.-S. Kim, I.-S. Hwang, S.-J. Kim, C.-Y. Lee, J.-H. %J S. Lee, and A. B. Chemical, "CuO nanowire gas sensors for air quality control in automotive cabin," vol. 135, no. 1, pp. 298–303, 2008.

[36] K. Shanmugapriya and H. W. Kang, "Engineering pharmaceutical nanocarriers for photodynamic therapy on wound healing: Review," *Mater. Sci. Eng. C*, vol. 105, p. 110110, Dec. 2019, doi: 10.1016/j.msec.2019.110110.

[37] E. Ahmed, A. O. El-Gendy, M. R. Hamblin, and T. Mohamed, "The effect of femtosecond laser irradiation on the growth kinetics of Staphylococcus aureus: An in vitro study," *J. Photochem. Photobiol. B Biol.*, vol. 221, p. 112240, Aug. 2021, doi: 10.1016/j.jphotobiol.2021.112240.

[38] A. O. El-Gendy, A. Samir, E. Ahmed, C. S. Enwemeka, and T. Mohamed, "The antimicrobial effect of 400 nm femtosecond laser and silver nanoparticles on gram-positive and gram-negative bacteria," *J. Photochem. Photobiol. B Biol.*, vol. 223, p.

112300, Oct. 2021, doi: 10.1016/j.jphotobiol.2021.112300.

[39] A. O. El-Gendy *et al.*, "Preparation of zinc oxide nanoparticles using laser-ablation technique: Retinal epithelial cell (ARPE-19) biocompatibility and antimicrobial activity when activated with femtosecond laser," *J. Photochem. Photobiol. B Biol.*, vol. 234, p. 112540, Sep. 2022, doi: 10.1016/j.jphotobiol.2022.112540.

[40] A. O. El-Gendy, Y. Obaid, E. Ahmed, C. S. Enwemeka, M. Hassan, and T. Mohamed, "The Antimicrobial Effect of Gold Quantum Dots and Femtosecond Laser Irradiation on the Growth Kinetics of Common Infectious Eye Pathogens: An In Vitro Study," *Nanomaterials*, vol. 12, no. 21, p. 3757, Oct. 2022, doi: 10.3390/nano12213757.

[41] S. S. Pavithran *et al.*, "Silver and Copper nano-colloid generation via Pulsed Laser Ablation in Liquid: Recirculation nanoparticle production mode," 2021.

[42] A. Neumeister, J. Jakobi, C. Rehbock, J. Moysig, and S. %J P. C. C. P. Barcikowski, "Monophasic ligand-free alloy nanoparticle synthesis determinants during pulsed laser ablation of bulk alloy and consolidated microparticles in water," vol. 16, no. 43, pp. 23671–23678, 2014.

[43] S. Mamdouh, A. Mahmoud, A. Samir, M. Mobarak, and T. %J P. B. C. M. Mohamed, "Using femtosecond laser pulses to investigate the nonlinear optical properties of silver nanoparticles colloids in distilled water synthesized by laser ablation," vol. 631, p. 413727, 2022.

[44] J. Zhang and C. Q. %J M. L. Lan, "Nickel and cobalt nanoparticles produced by laser ablation of solids in organic solution," vol. 62, no. 10–11, pp. 1521–1524, 2008.

[45] E. Ahmed, A. O. El-Gendy, N. A. Moniem Radi, and T. Mohamed, "The bactericidal efficacy of femtosecond laser-based therapy on the most common infectious bacterial pathogens in chronic wounds: an in vitro study," *Lasers Med. Sci.*, no. ii, 2020, doi: 10.1007/s10103-020-03104-0.

[46] J. Ghorbani, D. Rahban, S. Aghamiri, A. Teymouri, and A. Bahador, "Photosensitizers in antibacterial photodynamic therapy: an overview.," *Laser Ther.*, vol. 27, no. 4, pp. 293–302, Dec. 2018, doi: 10.5978/islsm.27_18-RA-01.

[47] C. M. Cassidy, M. M. Tunney, P. A. McCarron, and R. F. Donnelly, "Drug delivery strategies for photodynamic antimicrobial chemotherapy: From benchtop to clinical practice," *J. Photochem. Photobiol. B Biol.*, vol. 95, no. 2, pp. 71–80, May 2009, doi: 10.1016/j.jphotobiol.2009.01.005.

[48] X. Gu *et al.*, "Preparation and antibacterial properties of gold nanoparticles: a review," *Environ. Chem. Lett.*, vol. 19, no. 1, pp. 167–187, Feb. 2021, doi: 10.1007/s10311-020-01071-0.

[49] J. G. Hurdle, A. J. O'Neill, I. Chopra, and R. E. Lee, "Targeting bacterial membrane function: an underexploited mechanism for treating persistent infections," *Nat. Rev. Microbiol.*, vol. 9, no. 1, pp. 62–75, Jan. 2011, doi: 10.1038/nrmicro2474.

[50] S. C. Hayden *et al.*, "Aggregation and Interaction of Cationic Nanoparticles on Bacterial Surfaces," *J. Am. Chem. Soc.*, vol. 134, no. 16, pp. 6920–6923, Apr. 2012, doi: 10.1021/ja301167y.

[51] A. Simon-Deckers *et al.*, "Size-, Composition- and Shape-Dependent Toxicological Impact of Metal Oxide Nanoparticles and Carbon Nanotubes toward Bacteria," *Environ. Sci. Technol.*, vol. 43, no. 21, pp. 8423–8429, Nov. 2009, doi: 10.1021/es9016975.

[52] R. A. Gonçalves *et al.*, "Copper-Nanoparticle-Coated Fabrics for Rapid and Sustained Antibacterial Activity Applications," *ACS Appl. Nano Mater.*, vol. 5, no. 9, pp. 12876–12886, Sep. 2022, doi: 10.1021/acsanm.2c02736.

[53] A. Fazal, S. Ara, M. T. Ishaq, and K. Sughra, "Green Fabrication of Copper Oxide Nanoparticles: A Comparative Antibacterial Study Against Gram-Positive and Gram-Negative Bacteria," *Arab. J. Sci. Eng.*, vol. 47, no. 1, pp. 523–533, Jan. 2022, doi: 10.1007/s13369-021-05767-5.

[54] A. Azam, "Size-dependent antimicrobial properties of CuO nanoparticles against Gram-positive and -negative bacterial strains," *Int. J. Nanomedicine*, p. 3527, Jul. 2012, doi: 10.2147/IJN.S29020.

[55] "Nanotechnology for infectious diseases," *Nat. Nanotechnol.*, vol. 16, no. 4, pp. 1–1, Apr. 2021, doi: 10.1038/s41565-021-00909-0.

[56] C. N. Fries, E. J. Curvino, J.-L. Chen, S. R. Permar, G. G. Fouda, and J. H. Collier, "Advances in nanomaterial vaccine strategies to address infectious diseases impacting global health," *Nat. Nanotechnol.*, vol. 16, no. 4, pp. 1–14, Apr. 2021, doi: 10.1038/s41565-020-0739-9.